ChemComm

COMMUNICATION

View Article Online
View Journal | View Issue

Cite this: *Chem. Commun.*, 2018, **54**, 8198

Received 31st May 2018,
Accepted 21st June 2018

DOI: 10.1039/c8cc04334e

rsc.li/chemcomm

Supramolecular chemotherapeutic drug constructed from pillararene-based supramolecular amphiphile†

Dan Wu, ‡[a] Yang Li,‡[a] Jie Shen,*[b] Zaizai Tong,[c] Qinglian Hu,[d] Liping Li[e] and Guocan Yu *[a]

Based on the host–guest interaction between a CPT-conjugated prodrug amphiphile (CPT-ss-Py) and a water-soluble pillar[5]arene (P5), a GSH-responsive supramolecular chemotherapeutic drug (P5⊃CPT-ss-Py) was fabricated. Through this supramolecular formulation, internalization and anticancer efficacy were greatly increased.

Being able to modify the pharmacokinetic properties of drugs, improve the therapeutic efficacy and reduce side effects, nanomedicines have been attracting more and more attention from scientists over the past few years.[1] The first generation of nanomedicines have already obtained widespread clinical approval during the last couple of decades, from liposomal doxorubicin (Doxil) in 1995 to liposomal irinotecan (Onivyde) in 2015.[2] Even though several active anti-tumor drugs have been fabricated into the approved nanomedicines in the clinic,[3] there are still a number of drugs exhibiting remarkable preclinical anti-tumor activity urgently needed to be developed into nano-formulations. Camptothecin (CPT), an effective DNA topoisomerase I inhibitor, has been proven to possess outstanding anticancer activity, yet is unable to be applied in clinical trials owing to its severe side effects and low solubility.[4] Because of medium polarity and an inherently planar structure that can induce strong π–π stacking effect, CPT is also not easily encapsulated in the hydrophobic core of nanoparticles.[5] Hence, continuing efforts should be made towards highly efficient CPT delivery, especially focusing on nanoscale drug delivery systems (DDSs).

Owing to their high drug-loading ability, no premature/leaky drug release and simple manufacturing process, scientists have paid a great deal of attention to polymer–drug conjugates in recent years. Several polymer–drug conjugates have been investigated in clinical trials, such as dextran–doxorubicin in phase I, polyglutamate–paclitaxel in phase III, *N*-(2-hydroxypropyl)methacrylamide copolymer–CPT in phase I, *etc.*[6] However, uncontrollable modifications and inefficient drug release are still the great challenges for their clinical translation. Supramolecular chemistry is based on intermolecular interactions, namely on the connection of two or more building blocks which are linked together through non-covalent interactions.[7] Benefiting from a dynamic and reversible nature, supramolecular architectures possess outstanding stimuli-responsive properties and near-infinite possibilities. Among a variety of non-covalent interactions, such as π–π stacking interactions, charge-transfer interactions, electrostatic interactions, hydrogen bonds and host–guest interactions,[8] host–guest interactions are drawing an increasing amount of attention. By making use of supramolecular formulations, some limitations impeding polymer–drug conjugates for clinical applications could be solved efficiently. For example, easy functionalization can be achieved for supramolecular chemotherapeutic systems through simple modification of each building block. Premature drug release is inhibited during blood circulation and the loaded drugs are specifically released at tumor sites triggered by tumor microenvironment abnormalities, such as pH, enzymes, redox and temperature. As an indispensable part of host–guest interactions, macrocyclic host molecules usually consist of crown ethers,[9] calix[*n*]arenes,[10] cyclodextrins,[11] cucurbit[*n*]urils[12] and pillar[*n*]arenes.[13] Among them, pillar[*n*]arenes have become popular macrocyclic hosts in supramolecular chemistry since 2008 arising from their highly symmetrical and rigid structures, fruitful

[a] *Department of Chemistry, Zhejiang University, Hangzhou 310027, P. R. China. E-mail: guocanyu@zju.edu.cn*
[b] *School of Medicine, Zhejiang University City College, Hangzhou 310015, P. R. China. E-mail: shenj@zucc.edu.cn*
[c] *Key Laboratory of Advanced Textile Materials and Manufacturing Technology (ATMT), Ministry of Education, Department of Materials Science and Engineering, Zhejiang Sci-Tech University, Hangzhou 310018, P. R. China*
[d] *College of Biotechnology and Bioengineering, Zhejiang University of Technology, Hangzhou 310014, P. R. China*
[e] *Section on Medical Neuroendocrinology, Eunice Kennedy Shriver National Institute of Child Health and Human Development, National Institutes of Health, Bethesda, Maryland, USA*

† Electronic supplementary information (ESI) available: ^{1}H NMR, 2D NOESY spectra, ITC investigation and cytotoxicity evaluation. See DOI: 10.1039/c8cc04334e

‡ These authors contributed equally to this work.

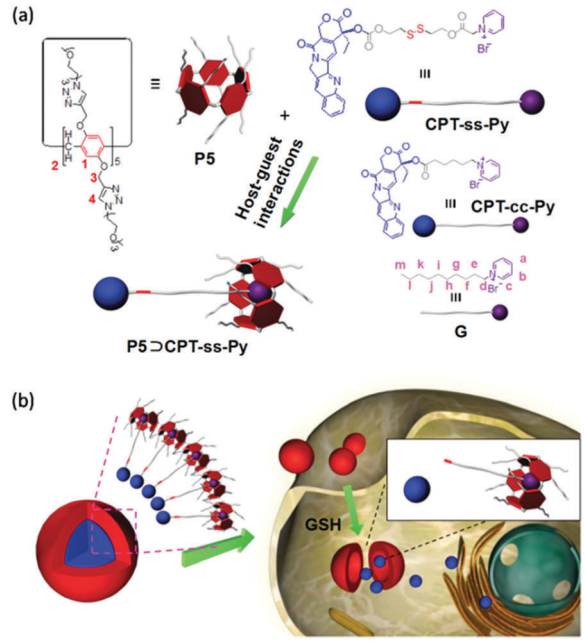

Scheme 1 (a) Structures of chemicals (**G**, **P5**, **CPT-cc-Py**, **CPT-ss-Py** and **P5⊃CPT-ss-Py**) and (b) schematic diagram for the formation of therapeutic supramolecular amphiphile **P5⊃CPT-ss-Py**.

host–guest chemistry and sophisticated functionalizations.[14] Their unique properties endow them with outstanding abilities to selectively couple different types of guests, providing opportunities to establish smart supramolecular DDSs.

Herein, we develop a therapeutic supramolecular amphiphile (**P5⊃CPT-ss-Py**) using a pillar[5]arene-based host–guest molecular recognition motif constructed from a pyridinium salt derivative (**G**) and a water-soluble pillar[5]arene (**P5**), mainly driven by cation–π and hydrophobic interactions (Scheme 1). Different from **CPT-ss-Py** that forms large aggregates, **P5⊃CPT-ss-Py** self-assembles into supramolecular nanoparticles (SNPs) with a mean diameter of about 150 nm in aqueous solution, which is favorable for cellular endocytosis. After the SNPs are internalized by cancer cells, the high-concentration glutathione (GSH) inside cancer cells rapidly cleaves the disulfide bond of **CPT-ss-Py**, resulting in the release of active CPT through a GSH-triggered cascade reaction. Through this supramolecular strategy, the internalization of **CPT-ss-Py** is significantly increased and the anticancer efficacy of CPT is greatly maintained.

^{1}H NMR spectroscopy was used to study the host–guest complexing action between pillar[5]arene (**P5**) and the model compound (*N*-decylpyridinium bromide, **G**). As shown in Fig. 1b and c, when equimolar amounts of **P5** and **G** were mixed in solution, changes of chemical shift of the protons on **G** were observed. For example, the signals corresponding to the protons $H_{a–c}$ of **G** displayed obvious upfield shifts (Fig. 1b and c), providing convincing evidence for the host–guest interaction between **P5** and **G**. The reason for the change in chemical shift was that protons $H_{a–c}$ were situated in the cavum of **P5** and screened by the electron-rich aromatic ring upon generation of the inclusion complex from **P5** and **G**.[15] Moreover, the signals

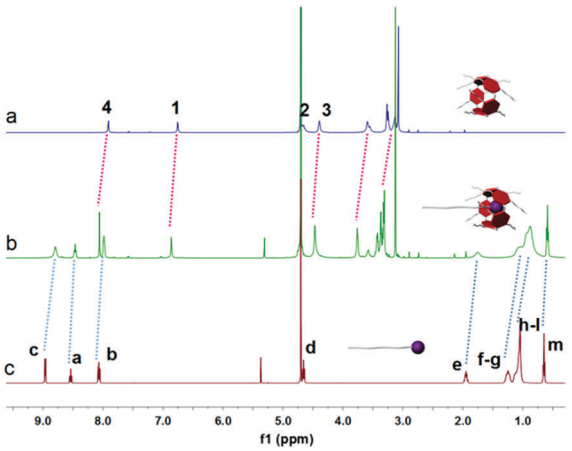

Fig. 1 Partial ^{1}H NMR spectra (D_2O, room temperature, 400 MHz): (a) **P5** (2.00 mM); (b) **P5** (2.00 mM) and **G** (2.00 mM); (c) **G** (2.00 mM).

related to protons $H_{1–4}$ on **P5** also showed apparent chemical shift changes induced by the host–guest complexation (Fig. 1a and b). On the other hand, Nuclear Overhauser effect correlation signals between H_1 of **P5** and H_c, $H_{f–l}$ and H_m of **G** were observed (Fig. S9, ESI†), further suggesting that **G** was threaded through the cavum of **P5**, coinciding with the results acquired from ^{1}H NMR investigations. Isothermal titration calorimetry (ITC) experiment was conducted to obtain thermodynamic energy information for the inclusion complexation between **P5** and **G**. As can be seen in Fig. S10 (ESI†), the K_a value of **P5⊃G** was determined to be $(2.00 \pm 0.30) \times 10^4$ M^{-1} and the complexation stoichiometry is 1 : 1. The driving forces of this supramolecular system should be ascribed to the combined actions of π–π stacking interactions, hydrophobic interactions and cation–π interactions between the electron-deficient **G** and electron-rich **P5**.[16] Besides, the entropy and enthalpy changes were also acquired from the ITC experiment ($\Delta H^\circ < 0$; $T\Delta S^\circ > 0$), demonstrating that this host–guest inclusion complexation was driven by a favorable enthalpy change assisted by entropy (Fig. S10, ESI†).

With this molecular recognition motif in hand, we further used it to establish a supramolecular amphiphile and studied the relevant self-assembly behavior in water. **CPT-ss-Py** containing a GSH-cleavable disulfide bond was employed as a therapeutic guest, where the anticancer drug CPT acted as the hydrophobic part and the pyridinium salt unit worked as the hydrophilic head. By measuring concentration-dependent conductivity, the critical aggregation concentration (CAC) of **CPT-ss-Py** was calculated to be about 1.72×10^{-6} M (Fig. 2a). In the presence of host molecule **P5**, the supramolecular amphiphile **P5⊃CPT-ss-Py** was formed, in which triethylene glycol-functionalized pillar[5]arene head acted as the hydrophilic part and the disulfide bond-containing CPT prodrug chain served as the hydrophobic portion. The CAC of **P5⊃CPT-ss-Py** increased to 3.21×10^{-6} M because of the formation of the stable host–guest complex between **P5** and **CPT-ss-Py** (Fig. 2b). It should be noted that partial host–guest complexation could change the CAC values and morphologies of the self-assemblies by altering the curvature of the membrane.[13d,15c,17] Transmission electron microscopy (TEM) assisted in the

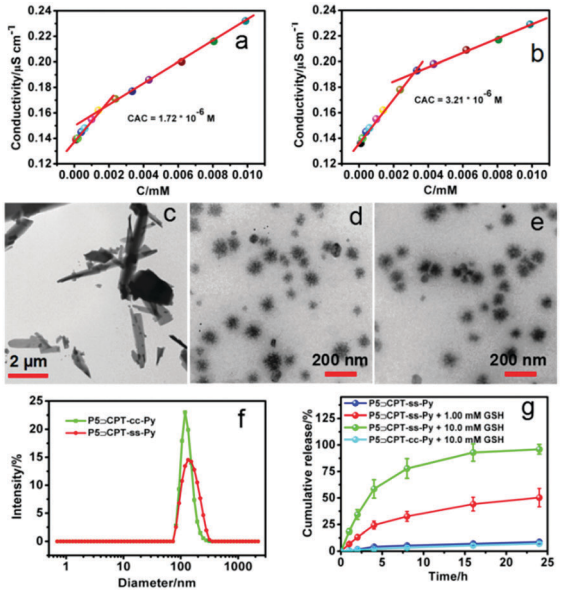

Fig. 2 The concentration-dependent conductivity of (a) **CPT-ss-Py** and (b) **P5⊃CPT-ss-Py**. TEM images of the sheet-like structure formed from (c) **CPT-ss-Py** and nanoparticles self-assembled from (d) **P5⊃CPT-ss-Py** and (e) **P5⊃CPT-cc-Py**. (f) DLS size distributions of nanoparticles self-assembled from **P5⊃CPT-cc-Py** and **P5⊃CPT-ss-Py**. (g) Drug release profiles of **P5⊃CPT-ss-Py** and **P5⊃CPT-cc-Py** with different concentrations of GSH.

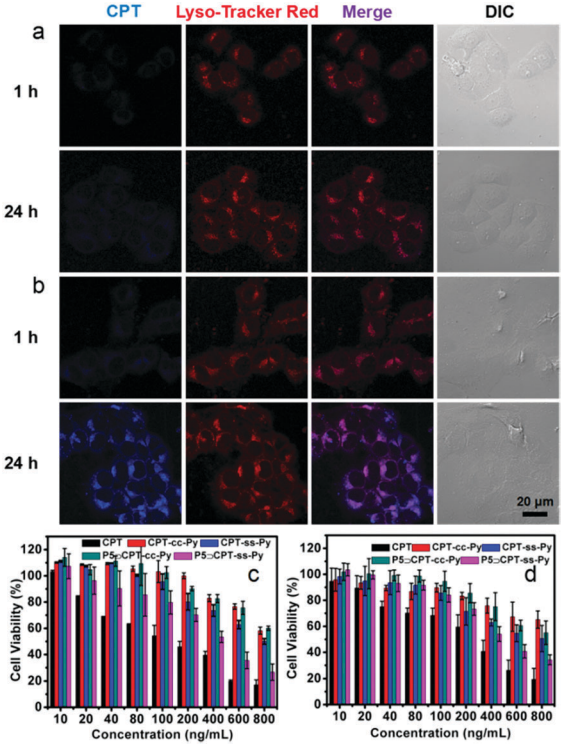

Fig. 3 Confocal images of HeLa cells incubated with (a) **CPT-ss-Py** and (b) **P5⊃CPT-ss-Py** for different time periods. Cytotoxicity against (c) HeLa and (d) A549 cells incubated with different concentrations of CPT, **CPT-cc-Py**, **CPT-ss-Py**, **P5⊃CPT-cc-Py** and **P5⊃CPT-ss-Py** for 24 h.

identification of the self-assembly morphologies of **CPT-ss-Py** and **P5⊃CPT-ss-Py**. As can be seen in Fig. 2c, **CPT-ss-Py** alone self-assembled into sheet-like structure (>2 μm) in water driven by the π–π stacking interactions between CPT tails. However, upon addition of **P5**, the sheet-like structure transformed into petal-shaped nanoparticles with diameters of about 130 nm (Fig. 2d). Dynamic light scattering (DLS) experiments were performed to measure the size of the nanoparticles. The average diameter of the self-assembled nanoparticles of **P5⊃CPT-ss-Py** was measured to be 152 nm (Fig. 2f), in good accordance with the TEM image. As a control, the TEM and DLS characterization experiments of **P5⊃CPT-cc-Py** were also conducted. As can be seen in Fig. 2f, the average diameter of **P5⊃CPT-cc-Py** was 127 nm, which is consistent with TEM image (Fig. 2e).

In the human body, the concentration of intracellular GSH (1–10 mM) is much higher than that in common body fluids outside cells (20–40 μM), such as plasma. Moreover, the concentration of intracellular GSH in cancer cells is much higher than that in normal cells.[18] In order to avoid side effects on normal cells and maintain the anticancer efficacy, disulfide bond was incorporated into this supramolecular amphiphile. The drug release profiles of **P5⊃CPT-ss-Py** under different GSH concentrations were evaluated, where the non-cleavable **P5⊃CPT-cc-Py** was used as a control. As shown in Fig. 2g, in the absence of GSH, only 8.8% CPT was released from **P5⊃CPT-ss-Py** within 24 h, indicating these SNPs were very stable under physiological condition. However, 50.3% and 95.9% CPT were released from **P5⊃CPT-ss-Py** SNPs respectively, in the presence of 1.0 and 10.0 mM GSH, confirming the GSH-triggered disassembly of the SNPs. As expected, only 7.2% CPT was released from **CPT-cc-Py** after 24 h, which further demonstrated the GSH-responsive feature of **P5⊃CPT-ss-Py**.

The internalization behavior of **P5⊃CPT-ss-Py** SNPs was further studied by confocal laser scanning microscopy (CLSM) using HeLa cells. As shown in Fig. 3b, slight blue fluorescence arising from CPT was observed in the cytoplasm after 1 h incubation, demonstrating that **P5⊃CPT-ss-Py** SNPs were internalized by HeLa cells. With the incubation time extended to 24 h, the blue fluorescence increased significantly, indicating the endocytosis of SNPs by HeLa cells occurred in a time-dependent manner. Furthermore, there was obvious purple fluorescence in the overlapped image, suggesting **P5⊃CPT-ss-Py** SNPs colocalized with lysosomes after entering into tumor cells. On the contrary, there was no clear blue fluorescence in the cytoplasm for **CPT-ss-Py** group even after 24 h incubation (Fig. 3a), because the size of the aggregates was too large. These data emphasized that this supramolecular modification played a significant role in increasing cellular uptake and the consequent anticancer efficacy.

Then the therapeutic efficacy of SNPs fabricated from **P5⊃CPT-ss-Py** was assessed by 3-(4′,5′-dimethylthiazol-2′-yl)-2,5-diphenyltetrazolium bromide (MTT) assay against HeLa, A549 and B16F10 cells, wherein the cells were treated with various concentrations of free CPT, **CPT-cc-Py**, **CPT-ss-Py**, **P5⊃CPT-cc-Py** and **P5⊃CPT-ss-Py**. As can be seen in Fig. 3c, compared with **P5⊃CPT-cc-Py**, **P5⊃CPT-ss-Py** was able to induce obvious cell death, indicating that the intracellular

reducing environment of tumor cells played an important role in the CPT release from SNPs. The IC_{50} value of **P5⊃CPT-ss-Py** against HeLa cells was 423 ng mL^{-1}, which could rival that of the anticancer drug CPT (137 ng mL^{-1}), much lower than those of **CPT-ss-Py** and **CPT-cc-Py**, demonstrating that the high-efficiency supramolecular chemotherapeutic drug **P5⊃CPT-ss-Py** and the cleavable disulfide bond of **CPT-ss-Py** are vital for excellent anticancer efficacy. It is worth noting that negligible influence on the relative cell viability was observed with concentrations of **CPT-cc-Py** and **CPT-ss-Py** ranging from 10 to 100 ng mL^{-1}. The reason was that the size of the sheet-like structures was too large such that they were hardly internalized by cells, which was proved by CLSM studies. A similar phenomenon was also observed for the other two types of cancer cell lines, namely A549 (Fig. 3d) and B16F10 (Fig. S11, ESI†), further indicating the robust anticancer behavior of **P5⊃CPT-ss-Py**.

In summary, a therapeutic supramolecular amphiphile was constructed based on a host–guest molecular recognition motif, in which a neutral water-soluble pillar[5]arene (**P5**) acted as the host and a CPT-conjugated pyridinium salt (**G**) worked as the guest. Benefiting from supramolecular formulation, **P5⊃CPT-ss-Py** self-assembled into stable SNPs with an average diameter of 152 nm in aqueous solution. In a high GSH environment, the disulfide bond was cleaved, resulting in the fast release of active CPT in cancer cells. CLSM experiments proved that these SNPs effectively enhanced the CPT uptake. MTT experiments revealed that not only was the efficacy of SNPs greatly maintained, but also they could perform well in other kinds of cancer cells, demonstrating the role of SNPs is a broad-spectrum one. The current study supplies a novel supramolecular method for the fabrication of stimuli-responsiveness DDSs, which has great potential for applications in cancer treatment.

This work was supported by the Fundamental Research Funds for the Central Universities.

Conflicts of interest

There are no conflicts to declare.

Notes and references

1 (*a*) K. Riehemann, S. W. Schneider, T. A. Luger, B. Godin, M. Ferrari and H. Fuchs, *Angew. Chem., Int. Ed.*, 2009, **48**, 872–897; (*b*) Z. Cheng, A. A. Zaki, J. Z. Hui, V. R. Muzykantov and A. Tsourkas, *Science*, 2012, **338**, 903–910; (*c*) S. Mura, J. Nicolas and P. Couvreur, *Nat. Mater.*, 2013, **12**, 991–1003; (*d*) G. Yu, M. Zhang, M. L. Saha, Z. Mao, J. Chen, Y. Yao, Z. Zhou, Y. Liu, C. Gao, F. Huang, X. Chen and P. J. Stang, *J. Am. Chem. Soc.*, 2017, **139**, 15940–15949; (*e*) S. K. Samanta, J. Quigley, B. Vinciguerra, V. Briken and L. Isaacs, *J. Am. Chem. Soc.*, 2017, **139**, 9066–9074; (*f*) L. Gao, T. Wang, K. Jia, X. Wu, C. Yao, W. Shao, D. Zhang, X.-Y. Hu and L. Wang, *Chemistry*, 2017, **23**, 6605–6614; (*g*) Q. Hao, Y. Chen, Z. Huang, J.-F. Xu, Z. Sun and X. Zhang, *ACS Appl. Mater. Interfaces*, 2018, **10**, 5365–5372; (*h*) G. Yu, Z. Yang, X. Fu, B. C. Yung, J. Yang, Z. Mao, L. Shao, B. Hua, Y. Liu, F. Zhang, Q. Fan, S. Wang, O. Jacobson, A. Jin, C. Gao, X. Tang, F. Huang and X. Chen, *Nat. Commun.*, 2018, **9**, 766–778; (*i*) G. Yu, X. Zhao, J. Zhou, Z. Mao, X. Huang, Z. Wang, B. Hua, Y. Liu, F. Zhang, Z. He, O. Jacobson, C. Gao, W. Wang, C. Yu, X. Zhu, F. Huang and X. Chen, *J. Am. Chem. Soc.*, 2018, **140**, 8005–8019.

2 S. Tran, P.-J. DeGiovanni, B. Piel and P. Rai, *Clin. Transl. Med.*, 2017, **6**, 44–64.

3 (*a*) N. K. Ibrahim, N. Desai, S. Legha, P. Soon-Shiong, R. L. Theriault, E. Rivera, B. Esmaeli, S. E. Ring, A. Bedikian, G. N. Hortobagyi and J. A. Ellerhorst, *Clin. Cancer Res.*, 2002, **8**, 1038–1044; (*b*) Y. Barenholz, *J. Controlled Release*, 2012, **160**, 117–134; (*c*) H. A. Blair and E. D. Deeks, *Drugs*, 2015, **75**, 2017–2024.

4 (*a*) T. Fang, Y. Dong, X. Zhang, K. Xie, L. Lin and H. Wang, *Int. J. Pharm.*, 2016, **512**, 39–48; (*b*) Y. Wen, Y. Wang, X. Liu, W. Zhang, X. Xiong, Z. Han and X. Liang, *Cancer Biol. Med.*, 2017, **14**, 363–370.

5 (*a*) J. Cui, Y. Yan, Y. Wang and F. Caruso, *Adv. Funct. Mater.*, 2012, **22**, 4718–4723; (*b*) K. Liang, J. J. Richardson, H. Ejima, G. K. Such, J. Cui and F. Caruso, *Adv. Mater.*, 2014, **26**, 2398–2402.

6 (*a*) S. Danhauser-Riedl, E. Hausmann, H.-D. Schick, R. Bender, H. Dietzfelbinger, J. Rastetter and A.-R. Hananske, *Invest. New Drugs*, 1993, **11**, 187–195; (*b*) N. Sarapa, M. R. Britto, W. Speed, M. Jannuzzo, M. Breda, C. A. James, M. Porro, M. Rocchetti, A. Wanders, H. Mahteme and P. Nygren, *Cancer Chemother. Pharmacol.*, 2003, **52**, 424–430.

7 (*a*) X. Zhang and C. Wang, *Chem. Soc. Rev.*, 2011, **40**, 94–101; (*b*) X. Yan, F. Wang, B. Zheng and F. Huang, *Chem. Soc. Rev.*, 2012, **41**, 6042–6065; (*c*) Y.-K. Tian, Y.-G. Shi, Z.-S. Yang and F. Wang, *Angew. Chem., Int. Ed.*, 2014, **53**, 6090–6094; (*d*) L. Yang, X. Tan, Z. Wang and X. Zhang, *Chem. Rev.*, 2015, **115**, 7196–7239.

8 (*a*) L.-Y. Niu, Y.-S. Guan, Y.-Z. Chen, L.-Z. Wu, C.-H. Tung and Q.-Z. Yang, *J. Am. Chem. Soc.*, 2012, **134**, 18928–18931; (*b*) G.-Z. Zhao, L.-J. Chen, W. Wang, J. Zhang, G. Yang, D.-X. Wang, Y. Yu and H.-B. Yang, *Chemistry*, 2013, **19**, 10094–10100.

9 (*a*) Z. Niu and H. W. Gibson, *Chem. Rev.*, 2009, **109**, 6024–6046; (*b*) G. J. E. Davidson, S. Sharma and S. J. Loeb, *Angew. Chem., Int. Ed.*, 2010, **49**, 4938–4942; (*c*) W. Jiang, A. Schäfer, P. C. Mohr and C. A. Schalley, *J. Am. Chem. Soc.*, 2010, **132**, 2309–2320; (*d*) Z. Niu, F. Huang and H. W. Gibson, *J. Am. Chem. Soc.*, 2011, **133**, 2836–2839.

10 I. E. Philip and A. E. Kaifer, *J. Am. Chem. Soc.*, 2002, **124**, 12678–12679.

11 (*a*) A. Mirzoian and A. E. Kaifer, *Chem. Commun.*, 1999, 1603–1604; (*b*) X. Liao, G. Chen, X. Liu, W. Chen, F. Chen and M. Jiang, *Angew. Chem., Int. Ed.*, 2010, **49**, 4409–4413.

12 (*a*) M. Ong, M. Gómez-Kaifer and A. E. Kaifer, *Org. Lett.*, 2002, **4**, 1791–1794; (*b*) Y. J. Jeon, H. Kim, S. Jon, N. Selvapalam, D. H. Oh, I. Seo, C.-S. Park, S. R. Jung, D.-S. Koh and K. Kim, *J. Am. Chem. Soc.*, 2004, **126**, 15944–15945.

13 (*a*) W. Si, Z.-T. Li and J.-L. Hou, *Angew. Chem., Int. Ed.*, 2014, **53**, 4578–4581; (*b*) N. L. Strutt, H. Zhang, S. T. Schneebeli and J. F. Stoddart, *Acc. Chem. Res.*, 2014, **47**, 2631–2642; (*c*) Z.-Y. Li, Y. Zhang, C.-W. Zhang, L.-J. Chen, C. Wang, H. Tan, Y. Yu, X. Li and H.-B. Yang, *J. Am. Chem. Soc.*, 2014, **136**, 8577–8589; (*d*) Y. Cao, X.-Y. Hu, Y. Li, X. Zou, S. Xiong, C. Lin, Y.-Z. Shen and L. Wang, *J. Am. Chem. Soc.*, 2014, **136**, 10762–10769.

14 (*a*) Y. Chang, K. Yang, P. Wei, S. Huang, Y. Pei, W. Zhao and Z. Pei, *Angew. Chem., Int. Ed.*, 2014, **53**, 13126–13130; (*b*) G. Yu, K. Jie and F. Huang, *Chem. Rev.*, 2015, **115**, 7240–7303; (*c*) L. Luo, G. Nie, D. Tian, H. Deng, L. Jiang and H. Li, *Angew. Chem., Int. Ed.*, 2016, **55**, 12713–12716; (*d*) B. Li, Z. Meng, Q. Li, X. Huang, Z. Kang, H. Dong, J. Chen, J. Sun, Y. Dong, J. Li, X. Jia, J. L. Sessler, Q. Meng and C. Li, *Chem. Sci.*, 2017, **8**, 4458–4464; (*e*) J. Zhou, G. Yu and F. Huang, *Chem. Soc. Rev.*, 2017, **46**, 7021–7053; (*f*) C. Sathiyajith, R. R. Shaikh, Q. Han, Y. Zhang, K. Meguellati and Y.-W. Yang, *Chem. Commun.*, 2017, **53**, 677–696; (*g*) S. Guo, Y. Song, Y. He, X.-Y. Hu and L. Wang, *Angew. Chem., Int. Ed.*, 2018, **57**, 3163–3167; (*h*) G. Yu, J. Yang, X. Fu, Z. Wang, L. Shao, Z. Mao, Y. Liu, Z. Yang, F. Zhang, W. Fan, J. Song, Z. Zhou, C. Gao, F. Huang and X. Chen, *Mater. Horiz.*, 2018, **5**, 429–435.

15 (*a*) C. Li, L. Zhao, J. Li, X. Ding, S. Chen, Q. Zhang, Y. Yu and X. Jia, *Chem. Commun.*, 2010, **46**, 9016–9018; (*b*) G. Yu, C. Han, Z. Zhang, J. Chen, X. Yan, B. Zheng, S. Liu and F. Huang, *J. Am. Chem. Soc.*, 2012, **134**, 8711–8717; (*c*) Q. Duan, Y. Cao, Y. Li, X. Hu, T. Xiao, C. Lin, Y. Pan and L. Wang, *J. Am. Chem. Soc.*, 2013, **135**, 10542–10549.

16 X. Chi, G. Yu, X. Ji, Y. Li, G. Tang and F. Huang, *ACS Macro Lett.*, 2015, **4**, 996–999.

17 K. Wang, D.-S. Guo, X. Wang and Y. Liu, *ACS Nano*, 2011, **5**, 2880–2894.

18 M. H. Lee, Z. Yang, C. W. Lim, Y. H. Lee, S. Dongbang, C. Kang and J. S. Kim, *Chem. Rev.*, 2013, **113**, 5071–5109.